

# The effect of ion-polymer binding on ionic diffusion in dicarbazole-based conducting polymers

Zvika Pomerantz<sup>a</sup>, Germà Garcia-Belmonte<sup>b,\*</sup>, Augustine Joseph<sup>a</sup>,  
Jean-Paul Lellouche<sup>a,\*</sup>, Juan Bisquert<sup>b</sup>, Arie Zaban<sup>a,\*</sup>

<sup>a</sup> Department of Chemistry, Bar-Ilan University, Ramat-Gan 52900, Israel

<sup>b</sup> Departament de Física, Universitat Jaume I, 12071 Castelló, Spain

Received 1 March 2007; received in revised form 19 April 2007; accepted 25 April 2007

Available online 10 May 2007

## Abstract

An electrochemical polymerization and characterization is reported on a series of eight dicarbazole-type conducting polymers with different attached functional groups. The influence of the electronic character of the subgroup on the ionic conductivity properties of the polymers was examined. Impedance spectroscopy measurements were used to set the ionic chemical diffusion coefficients,  $D$ , in the polymer matrix at a variety of doping levels, for each of the polydicarbazoles. We relate  $D$  dependency with potential to morphological and electronic processes in the polymer occurring during oxidation. By combination of cyclic voltammetry and impedance spectroscopy for part of the series we reveal that the diffusion of ions in the matrix is easier in polymers where the functional group is highly electron-attracting.

© 2007 Elsevier Ltd. All rights reserved.

**Keywords:** Polydicarbazole; Ionic diffusion; Cyclic voltammetry; Impedance spectroscopy; Conducting polymers

## 1. Introduction

The understanding of transport and doping of conducting polymers (CPs) is a subject of current interest in various fields joined by the common use of these polymers to improve exciting devices or form new applications. These devices typically involve their unique conductivity properties and the fact that they can be combined and used for many fields, including electronic applications (LEDs, batteries, photovoltaic cells and more) and microfabricated biosensing devices.

Electrochemical impedance spectroscopy (EIS) is one of the best techniques for analyzing the properties of conducting polymer electrodes and it has been broadly discussed in the literature using a variety of theoretical models [1,2]. In the case of electrochemical systems, EIS can reveal information regarding processes occurring in the polymer matrix when it is doped. This may include kinetic values of the doping processes and parameters of the diffusion of ions into the polymers. These processes

have a significant effect on the conductivity of the polymer, thus determination of values such as the chemical diffusion coefficient,  $D$ , as a function of the doping levels, provides better understanding of the conductivity mechanism. A combination of EIS with standard electrochemical methods such as cyclic voltammetry (CV), provides a powerful tool to understand the properties of CPs and thus to develop useful compounds for the specific applications [3].

The present communication reports on the effect of subgroups that are not part of the conducting chain on the polymer properties [4–7]. The study involves a series of eight dicarbazole monomers (labeled **I–VIII** in Table 1 and Fig. 1) that differ one from another by the electron-attracting character of the subgroup attached to the chain connecting the two carbazole units. The specific point of contact, the chiral center, induces asymmetry into the dicarbazole monomer. The motivation to synthesize this series and examine its electrochemical behavior originates from a previous study of dicarbazole **I**. Detailed analysis of the potentiodynamic behavior of dicarbazole **I** revealed a clear influence of the subgroup attached to the chiral center on the polymerization process and the potentiodynamic behavior in a monomer-free solution. In the case of dicarbazole **I**, the difference between the two carbazole units, which was evident in both

\* Corresponding authors.

E-mail addresses: [garcia@uji.es](mailto:garcia@uji.es) (G. Garcia-Belmonte),  
[lellouj@mail.biu.ac.il](mailto:lellouj@mail.biu.ac.il) (J.-P. Lellouche), [zabana@mail.biu.ac.il](mailto:zabana@mail.biu.ac.il) (A. Zaban).

Table 1  
Subscript names and IUPAC names of **I–VIII** dicarbazoles

Subname	Functional group	IUPAC name
<b>I</b>	Activated ester	2,6-Bis-carbazol-9-yl-hexanoic acid pentafluorophenyl ester
<b>II</b>	Activated ester	2,6-Bis-carbazol-9-yl-hexanoic acid 2,5-dioxo-pyrrolidin-1-yl ester
<b>III</b>	Activated ester	2,6-Bis-carbazol-9-yl-hexanoic acid 1,3-dioxo-1,3-dihydro-isindol-2-yl ester
<b>IV</b>	Methyl ester	2,6-Bis-carbazol-9-yl-hexanoic acid methyl ester
<b>V</b>	Free acid	2,6-Bis-carbazol-9-yl-hexanoic acid
<b>VI</b>	Acetate	2,6-Bis-carbazol-9-yl-hexan-1-ol acetate
<b>VII</b>	Chloromethyl	2,6-Bis-carbazol-9-yl-1-chlorohexane
<b>VIII</b>	Hydroxymethyl	2,6-Bis-carbazol-9-yl-hexan-1-ol

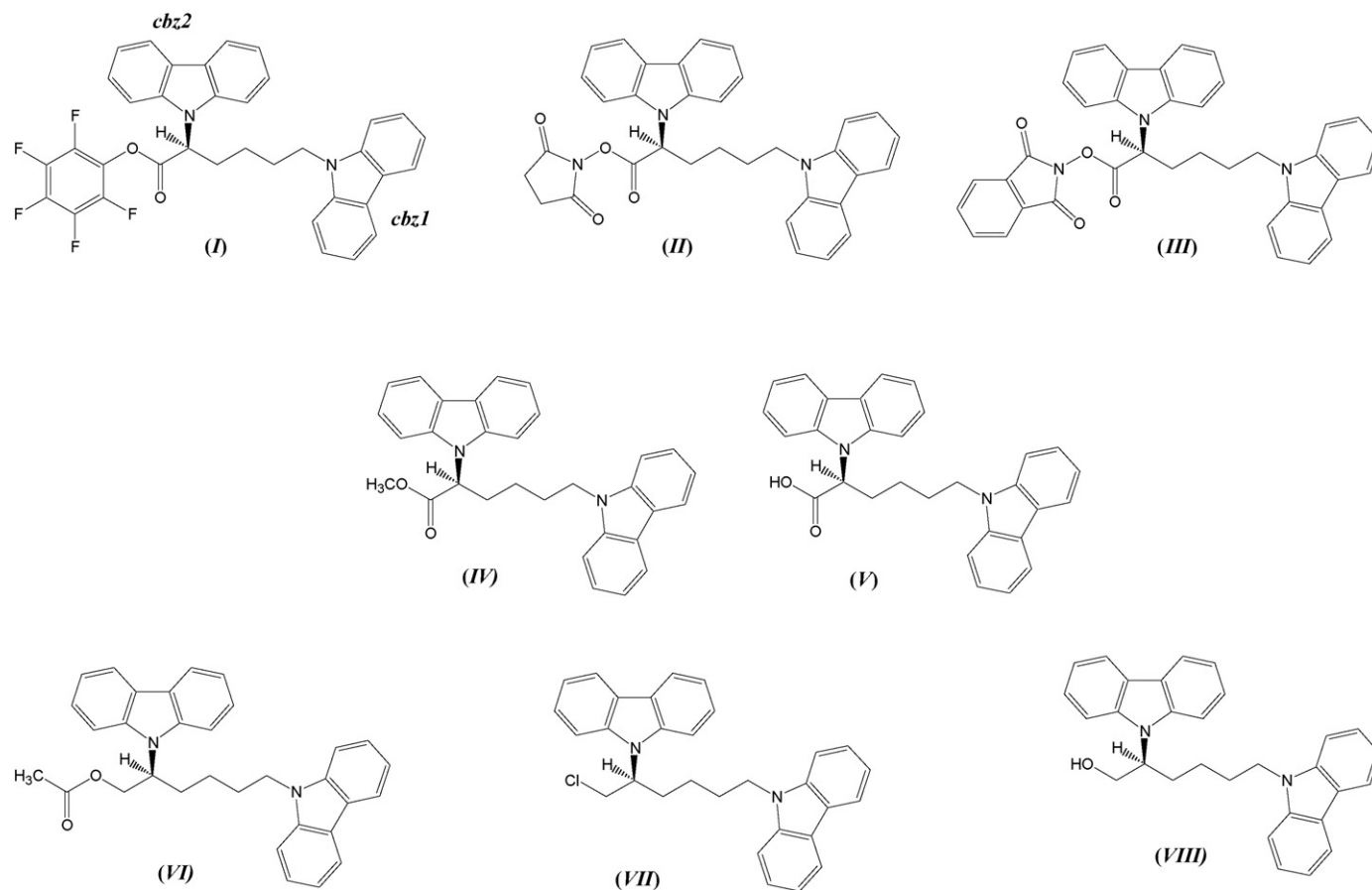


Fig. 1. Chemical structures of **I–VIII** dicarbazoles used in this study.

the polymerization and characterization CVs, was attributed to the electronegative nature of the subgroup [8]. The results show that concepts developed for dicarbazole **I** fit the whole series thus providing the evidence and general basis to these concepts. Furthermore, the series reveals a systematic effect of the electronegative nature of subgroups on the counter-ions diffusion into the polymer during the doping process.

## 2. Experimental

### 2.1. Synthesis of dicarbazole monomers (**I–VIII**)

The (*S*)-dicarbazole monomer **V** has been synthesized from commercially available (*L*)-Lysine monohydrochloride

using a modified Clauson-Kaas reaction [9] (2,5-dimethoxytetrahydrofuran (DMT), AcOH/dioxane, 1 h at 120 °C and overnight at 25 °C, enantiomeric enrichment better than 98%). It has been converted to corresponding activated esters **I–III** (R–OH, dicyclohexylcarbodiimide – DCC –, CH<sub>2</sub>Cl<sub>2</sub>, dimethylamino-4-pyridine – DMAP –, 2 h, 25 °C). A simple acid-catalyzed esterification performed in methanol afforded the methyl ester **IV** (methanol, catalytic conc. H<sub>2</sub>SO<sub>4</sub> acid, reflux, 1 h). This same methyl ester **IV** was also reduced using the alane diisobutylaluminium hydride (DIBAL, CH<sub>2</sub>Cl<sub>2</sub>, 25 °C, 2 h) toward the corresponding alcohol **VIII**, which was laterly chlorinated toward the methyl chloride **VII** using the PPh<sub>3</sub>/CCl<sub>4</sub> system (PPh<sub>3</sub>, CCl<sub>4</sub>, reflux, 10 h). Common acetylation of the methyl alcohol **VIII** at room temperature afforded the acetate

**VI** (Ac<sub>2</sub>O, pyridine, 25 °C, 2 h). All these compounds have been characterized using a range of analytical and spectroscopic methods (FT-IR, <sup>1</sup>H/<sup>13</sup>C NMR, CI and/or DCI/MS). Compound homogeneities were checked by thin-layer chromatography TLC and analytical HPLC when necessary.

We disclose here the characterization data of the acidic dicarbazole compound **V** as an example. All other characterizations are available as [Supplementary data](#).

(*S*)-2,6-Bis-carbazol-9-yl-hexanoic acid **V**. Pale yellow solid; mp: 157–158 °C (from hexane-CH<sub>2</sub>Cl<sub>2</sub>); FT-IR (KBr pellet, cm<sup>-1</sup>): 3446, 2929, 1714, 750, 723; <sup>1</sup>H NMR (CDCl<sub>3</sub>, 300 MHz): δ 8.15 (d, *J* = 7.8 Hz, 2H), 8.06 (d, *J* = 7.8 Hz, 2H), 7.39–7.15 (m, 12H), 5.20 (dd, *J* = 7.2, 4.8 Hz, 1H), 4.13–4.04 (m, 2H), 2.55–2.23 (m, 2H), 1.90–1.58 (m, 2H), 1.35–1.12 (m, 2H); <sup>13</sup>C NMR (CDCl<sub>3</sub>, 75 MHz): δ 173.7 (C=O), 140.1, 139.7, 125.8, 125.6, 123.3, 122.7, 120.5, 120.3, 119.8, 118.8, 109.3, 108.4, 56.3, 42.5, 29.1, 28.3, 24.1; MS (DCI, CH<sub>4</sub>): *m/z* 447 (27.6%, [MH]<sup>+</sup>), 446 (67.6%, [M]<sup>+</sup>), 402 (38.6%, [M-COO]<sup>+</sup>), 180 (100%); high-resolution MS (DCI, CH<sub>4</sub>) *m/z* calcd for C<sub>30</sub>H<sub>26</sub>N<sub>2</sub>O<sub>2</sub> [M]<sup>+</sup> 446.1994. Found 446.1964; [α]<sub>D</sub><sup>21</sup> = +11.7° (*c* = 0.01 gm L<sup>-1</sup>, CH<sub>2</sub>Cl<sub>2</sub>).

## 2.2. Electrochemistry part

All experiments were done in a glove box atmosphere (Ar, <1 ppm O<sub>2</sub>, <1 ppm H<sub>2</sub>O) in a three-electrode cell, connected to an Eco Chemie Autolab 20 potentiostat, where Pt electrode (1 mm Ø) serves as working electrode, an Ag/AgNO<sub>3</sub> as a reference electrode and a Pt ribbon as a counter electrode. All potentials are reported versus Ag/AgNO<sub>3</sub>. The experiments regarding each of the **I–VIII** dicarbazole series polymers include three parts: (a) electrochemical polymerization by successive cyclic voltammetry (CV), (b) characterization by CV in a monomer-free solution (typical CV) and (c) an electrochemical impedance spectroscopy study in a monomer-free electrolyte. Both the polymerizations and the typical CVs were done in 1:4 dichloromethane–acetonitrile solution (HPLC grade) containing 0.16 M of battery grade tetrabutylammonium perchlorate (TBAClO<sub>4</sub>) salt. For the polymerization 0.01 M of the monomer was added to the electrolyte. Each polymerization consisted of 10 scans between 0 and 1.2 V at 100 mV/s, typically the current in the polymerization region increased from one scan to

another, reflecting the polymer growth. Following the polymerization, the polymer coated Pt electrode was washed with a 1:4 dichloromethane–acetonitrile solution to remove monomers leftovers and placed in a monomer-free solution for typical CV characterization. The potential range and scan rate during the typical CV were similar to those used during the polymerization. The impedance spectroscopy measurements were done in a 0.2 M TBAClO<sub>4</sub>–acetonitrile solution under steady-state conditions achieved by the application of constant potential for 30 min prior to the measurement. The frequency range in the impedance measurements was 50 kHz–0.1 Hz.

## 3. Results and discussion

### 3.1. Electrochemical polymerization

Fig. 2 presents polymerization voltammograms of three dicarbazole monomers [10]. The voltammograms reflect two processes occurring at different potentials. The first peak, at ~600 mV (labeled as peak *p*), is associated with the oxidation of the polymer to its conductive state (doping). At higher potentials one finds either one peak (Fig. 2c, ~1000 mV) or two peaks (Fig. 2a, ~800 and ~1000 mV), which are assigned to the monomer oxidation. As the subgroup attached to the chiral center becomes more electron-attracting, the oxidation potential of the carbazole close to it (labeled as **cbz2**) is more positive and thus the oxidation peak in the CV is shifted positively. This phenomenon induces the difference between the two carbazole units of dicarbazole **I** (subgroup: pentafluorophenol ester) as shown in Fig. 2a. The oxidation potential of the carbazole labeled **cbz1** is lower by 250 mV compared with the oxidation potential of carbazole **2**. Following the same approach, the polymerization curve of dicarbazole **VIII**, which contains an electron-donor subgroup (alcohol) rather than an electron-attracting group (Fig. 2c), presents no difference between oxidation potentials of the two carbazoles units (**1** and **2**). Consequently, only one broad peak of monomers oxidation appears during the polymerization CV (~950 mV). Dicarbazoles containing low electron-attracting subgroups, present a minor difference between the oxidation of the two carbazoles, **cbz1** and **cbz2**, as one can find in the polymerization curve of dicarbazole **V** (Fig. 2b; subgroup: acid). All eight polymerization voltammograms of dicarbazoles **I–VIII**

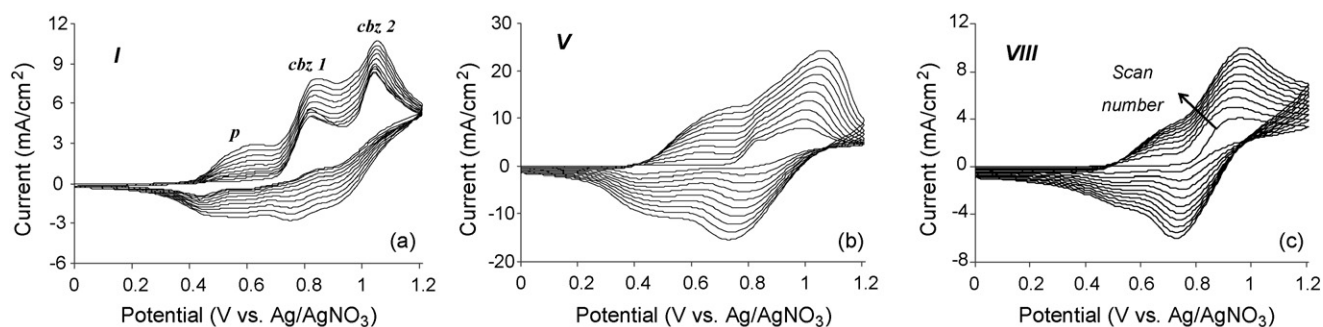


Fig. 2. Potentiodynamic growth of three polydicarbazoles (a–c relates to monomers **I**, **V** and **VIII**, respectively) with different electron-attracting character of the subgroups on the chiral center. At each curve the lowest peak (~600 mV) is the characteristic peak of the polymer and the higher potential(s) peak(s) relate to the monomer.

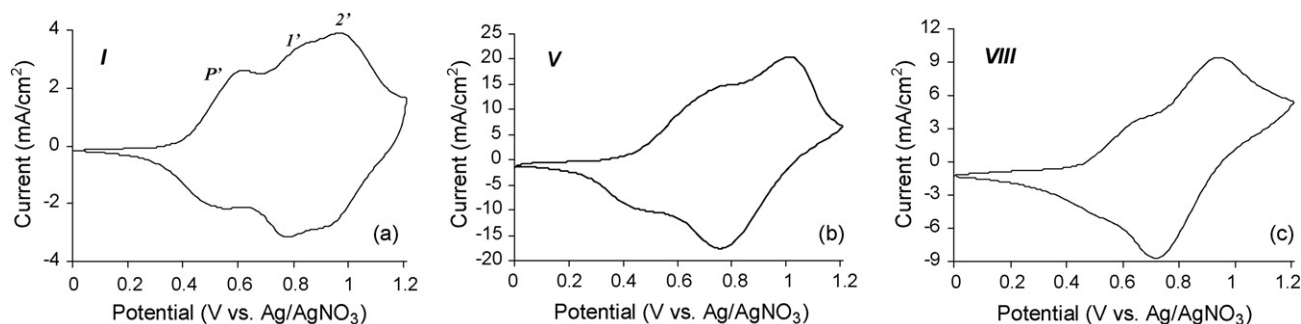


Fig. 3. Three typical cyclic voltammograms of the polydicarbazoles **I** (a), **V** (b) and **VIII** (c) films, in solution free of monomer showing two or three peaks, which is related to the polymer oxidation and to dangling carbazole units as described in the text.

present the same phenomena where the electron-attracting ability of the subgroup on the chiral center shifts the oxidation potential of the closer carbazole [11].

### 3.2. Electrochemical behavior of the polymer

The polydicarbazoles were electrochemically characterized in a monomer-free electrolyte. Fig. 3 presents the typical cyclic voltammograms for dicarbazole polymers poly(**I**), poly(**V**) and poly(**VIII**). The voltammograms show similar trends with respect to the potentiodynamic behavior during the polymer formation (Section 3.1). Here, also we attribute the low potential peaks (marked by  $p'$ ) to the polymer transition from insulator to conductor, while the latter (two) peak(s) are assigned to the oxidation of carbazole units that are connected to the polymer by the alkyl chain but are not part of the conducting network, i.e. dangling carbazoles. The polymerization process necessitates chaining of one carbazole unit per monomer. Most of the monomers are cross-linked by both carbazole units, however, one can expect a small fraction in which only one carbazole is polymerized [8,10]. This structure leads to sided dangling carbazole units of both types **1** and **2** having approximately the same oxidation potentials as the free monomer in solution. A small potential shift is, however, expected due to the physical connection of the carbazole unit to the polymer network. Indeed, a comparison of Figs. 2 and 3 shows that the onset potentials of the two high potential peaks are negatively shifted with respect to the corresponding peaks at the polymerization process [12].

The peak reflecting the oxidation of carbazole **2** (the carbazole closer to the chiral center) is shifting towards higher potentials with increasing electron-attracting ability of the subgroup attached to the chiral center. This is because increasing the electron-attraction of the subgroup makes carbazole **2** electron poorer which consequently shifts its oxidation potential positively. Therefore, the oxidation potential of carbazole **2**, can serve as an electron-attracting setting parameter.

Fig. 4 presents the  $E_{1/2}$  of the oxidation potential of carbazole **2** in the **I–VIII** polydicarbazoles series (we found the exact peak positions by its second derivatives while we always took the value of the highest potential peak; for polymers containing highly electron-attracting subgroup it reflects the oxidation potential of carbazole **2** and not the oxidation potential of carbazole **1**, while for polymers with low electron-attracting subgroup it reflects the

oxidation potentials of carbazole **2** and carbazole **1** as there is no difference between their oxidation potentials). The oxidation potential of carbazole **2**, in terms of  $E_{1/2}$  of the relevant peaks in the CV, follows the subgroup labeling (**I–VIII**), i.e. the relative electron-attracting ability of the subgroups that was estimated using general organic chemistry rules [13]. This electron-attracting ability order (**I** > **II** > **III** > **IV** > **V** > **VI** > **VII** > **VIII**) is the basis for the interpretation of the results in the following sections.

### 3.3. Electrochemical impedance spectroscopy

Electrochemical impedance response of electronically conducting polymers is known to be represented by a circuit model-containing interfacial as well as diffusion elements in cases where the polymer films are regarded as homogenous. In the simplest configuration, the impedance model considers a single (ionic) charge carrier diffusing along such an active film. This model includes several circuit elements that are related to the different transport and capacitive mechanisms involved in

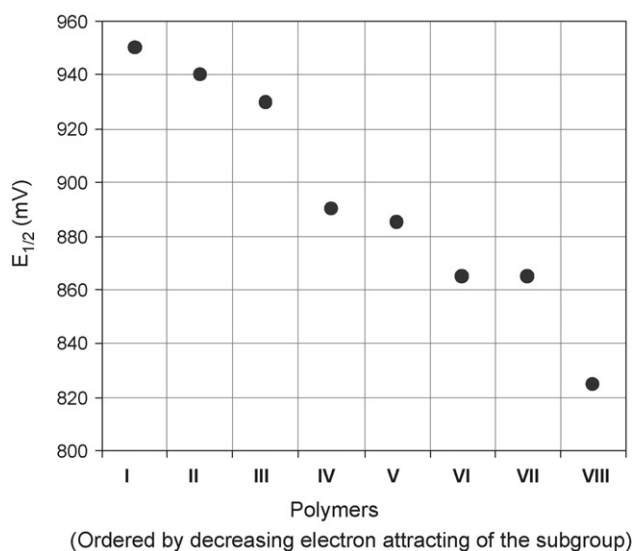


Fig. 4.  $E_{1/2}$  of carbazole **2** oxidation at **I–VIII** polydicarbazoles as a function of assumed electron-attracting ability of the subgroup on the chiral center. Higher electron-attracting groups shift the oxidation potentials of carbazole **2** toward higher potentials.

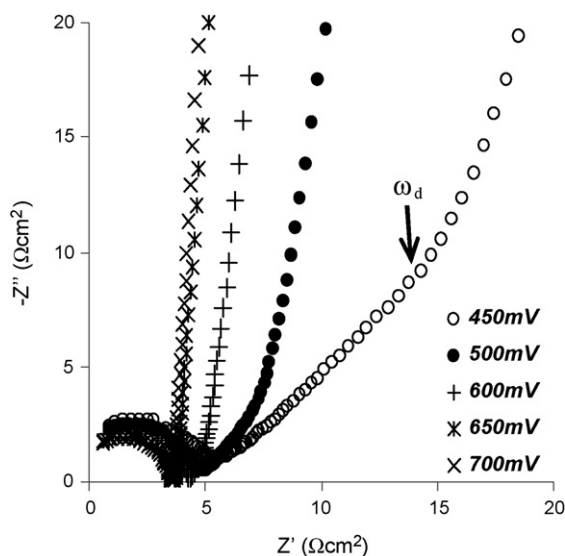


Fig. 5. Impedance spectra accepted for polydicarbazole **VIII** at five steady-state potentials. Anomalous diffusion behavior can be clearly seen. Each of **I–V** polymers exhibits anomalous diffusion behavior.

the polymer oxidation (doping): a series resistance,  $R_s$ , for the electrolyte and contacts contribution; a capacitance,  $C_{dl}$ , for the double-layer at the electrolyte-polymer film interface; an ionic charge transfer resistance,  $R_{ct}$ , and finally a diffusion element accounting for the ionic diffusion and charging of the film,  $Z_D$ . The spectra presented in Fig. 5, recorded for polydicarbazole **I** at several steady-state potentials, reflect the various elements of the model. The high-frequency wing of such spectra shows a small portion of an arc, which corresponds to the parallel combination of  $C_{dl}$  and  $R_{ct}$ . At lower frequencies ( $<10^3$  Hz), the spectra are dominated by the spatially restricted anomalous diffusion element  $Z_D$  given by [1]

$$Z_D = R_0 \left( \frac{i\omega}{\omega_d} \right)^{-\gamma/2} \coth \left[ \left( \frac{i\omega}{\omega_d} \right)^{\gamma/2} \right] \quad (1)$$

where  $\omega$  is the angular frequency,  $R_0$  the resistance associated with diffusion and  $\gamma$  relates to the deviation from the normal spatially restricted diffusion impedance ( $\gamma=1$ ). The diffusion impedances undergo a change of pattern at a certain character-

istic frequency,  $\omega_d$ , at which a transition between a Warburg- and a capacitive-like behavior is observed. The frequency  $\omega_d$  is located near the elbow of the impedance plot. Each polymer of the **I–VI** polydicarbazoles presents the anomalous diffusion pattern ( $\gamma < 1$ ) related to structural disorder effects, which generally occur in amorphous materials.

The method and principles for fitting the experimental results spectra to the anomalous diffusion model were published by us elsewhere [14]. The chemical diffusion coefficient  $D$  corresponding to the ionic motion is related to the characteristic frequency  $\omega_d$  as

$$\omega_d = \frac{D}{L^2} \quad (2)$$

where  $L$  represents the polymer film thickness measured as described elsewhere [15].

Different doping levels were established by application of dc bias within the potential range where the polymer is only partially conducting. Fig. 6a shows ionic diffusion coefficient values,  $D$ , of five polydicarbazoles (**I**, **II**, **III**, **IV**, **V**) as a function of the applied bias. For clarity, Fig. 6b presents the same data, only normalized to a value of 1 at their maximum. (Three polymers of the series are not presented in Fig. 6: polymer **VIII** did not exhibit a diffusion-like impedance response and therefore the determination of the chemical diffusion coefficient was impractical. Polymers **VI** and **VII** are not presented because the potential at which  $D_{peak}$  occurs is outside the electrochemical window measured). All polymers presented in Fig. 6 show a similar trend. The ionic diffusion coefficient,  $D$ , increases with potential to a maximum value after which additional bias results in a decrease of  $D$ . In other words, as the polymer doping progresses the diffusion of ions into the polymer enhances up to a certain doping level at which ionic diffusion becomes more difficult. The potential at which the maximum  $D$  is reached varies within the examined polymer series.

We attribute the peak-shaped dependence of  $D$  to two competing processes that are associated with the doping. The doping process, i.e. oxidation of the polymer, requires diffusion of negative ions from the solution into the polymer film in order to compensate the excess positive charge. At low potentials diffusion of the ions into the polymer matrix is structurally limited

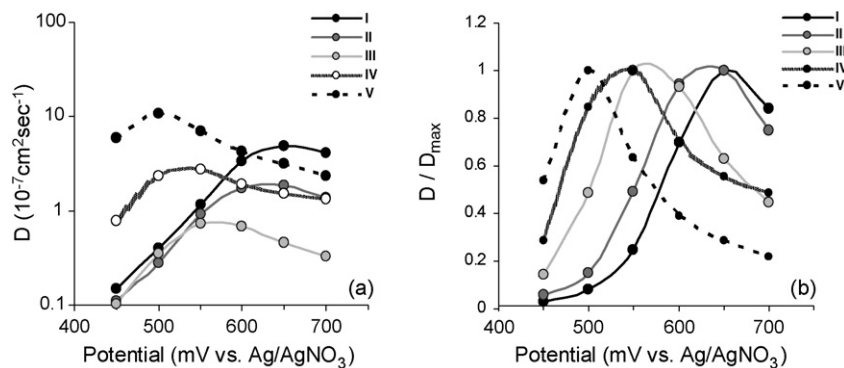


Fig. 6. The ionic diffusion coefficients for five polydicarbazoles. The values were accepted by fitting the impedance results to the anomalous diffusion model (a) and normalized to the highest value (b).

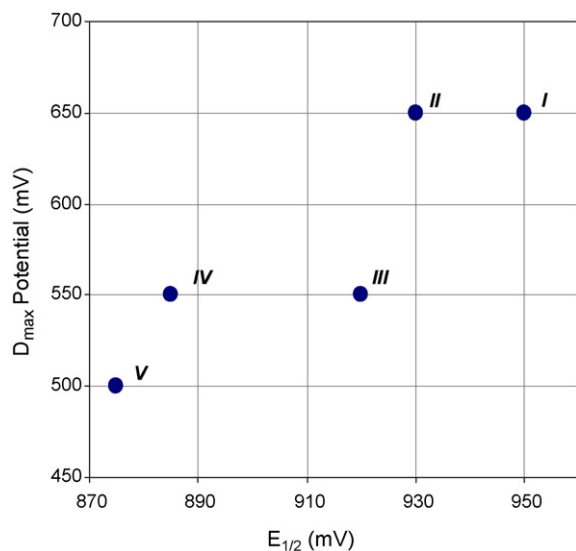


Fig. 7. The potential of where each polymer reaches  $D_{\max}$  is presented vs. its  $E_{1/2}$  value of carbazole **2**. The latter parameter serves as an electron-attracting ability parameter and its influence on the diffusion of ions in the polymer matrix is clear.

as the polymer morphology is changing from a compact to an opened one (swelling) [16,17]. Therefore, shifting the potential positively opens the matrix resulting in easier diffusion of the ions into the polymer, i.e.  $D$  increases. In contrast, the increasing concentration of negative ions inside the polymer associated with the positive shift of the applied potential slows the diffusion. The negative ions that entered the polymer matrix repel new ones from entering the matrix and their movement inside the oxidized polymer becomes more difficult, i.e.  $D$  decreases. The results presented in Fig. 6 shows that the diffusion determining process changes as doping progresses. At low doping levels, polymer opening is more significant, while ion repulsion takes the control at higher levels. The transformation between the two diffusion control processes occurs at the potentials associated with the diffusion maxima ( $D_{\text{peak}}$ ) in the presentation of Fig. 6. We note that the transition potential varies with the attached subgroup.

Fig. 7 presents the relation between the transformation potential ( $D_{\text{peak}}$  in Fig. 6) and the electron-attracting ability of the attached subgroup (described by  $E_{1/2}$  of the oxidation of carbazole **2**). We find that the stronger electron-attracting subgroups (higher  $E_{1/2}$ ) are associated with higher transformation ( $D_{\text{peak}}$ ) potentials. These results can be understood in terms of the different roles of counterions inside the matrix according to their transition in the polymer chain. It has been suggested [18] that counterions balancing the positive charge in the chain, experience different amounts of attraction towards the chain. First, there should be ions strongly attached to the conducting chain, and in addition, other ions should be less tightly bound and more mobile in the space between the polymer segments. At a given potential (doping level), some fraction of ions is strongly attached to the chains, i.e. these ions are trapped close to the chains, and by that implies a lower concentration of ions in the channel between the chains. At the latter zone, the coulombic

repulsion between the ions trapped near the chains and the ions in the channel is relatively low. Hence, the stronger the trapping of ions near the chains the lower the coulombic repulsion between them and ions in the channel. In the case of low coulombic repulsion between these two types of ions we expect easier diffusion of free ions in the channel, and vice versa. As the bias potential increases, bulk ions are required (to maintain electroneutrality). The diffusion of the latter depends on the coulombic repulsion in the polymer channel, and hence by the binding degree of the ions attached to the polymer chains.

Indeed our experimental results indicate that the repulsion effect as reflected by  $D_{\max}$ , is less dominant for polymers derivatized with strong electron-attracting subgroups. Oxidation of carbazole **2** to which a highly electron-attracting group is attached (e.g. poly-I) leads to stronger binding of the counterion, and the coulomb repulsion in the interchain channels is low, allowing easy diffusion of fresh ions up to high potentials, i.e.  $D_{\text{peak}}$  appears at high potentials. In the case of low electron-attracting subgroups polymers (i.e. poly-V) carbazole **2** is relatively electron-rich and the counter-ions are poorly bound to it. This leads to higher repulsion of bulk counter-ions in the channel between the polymer chains, and thus to lower values of  $D_{\text{peak}}$  potential. Therefore, Fig. 7 shows the effect of subgroups which are not part of the polymer and its electronic properties. We are aware that setting  $D_{\max}$  for more bias potentials (i.e. better than 50 mV resolution) could emphasize the trend presented in Fig. 7.

#### 4. Summary

We investigated the electrochemical behavior of eight poly-dicarbazole conducting polymers with different subgroups linked to the monomer chiral center. We found that the electron-attracting nature of the subgroup influences its electropolymerization characteristics and its typical cyclic voltammetry peak positions in monomer-free solution. The electrochemical behavior of the polymer in a monomer-free solution provides relative value of electron-attracting ability of the subgroup attached to carbazole **2** in terms of  $E_{1/2}$ .

Using anomalous diffusion model of impedance spectroscopy, we calculated the ionic diffusion coefficient of five polymers from the eight mentioned, at continued doping levels and we found that the electron-attracting/repelling nature of the subgroup attached to carbazole **2** influences the diffusion of anions from the solution in the matrix ( $D_{\text{ion}}$ ). We explain this behavior in terms of binding of the counter-ion to the oxidized carbazole: the higher the electron-attracting ability of the subgroup, the higher the binding of the counter-ion to carbazole **2** and thus the lower the coulombic repulsion of ions in the polymer matrix.

#### Acknowledgements

The work was supported by Ministerio de Educación y Ciencia of Spain under projects MAT2004-05168 and by the VIth Framework European project NACBO (Grant NMP3-2004-500802-2).

## Appendix A. Supplementary data

Supplementary data associated with this article can be found, in the online version, at [doi:10.1016/j.electacta.2007.04.118](https://doi.org/10.1016/j.electacta.2007.04.118).

## References

- [1] J. Bisquert, A. Compte, *J. Electroanal. Chem.* 499 (2001) 112.
- [2] M.D. Levi, Y. Gofer, D. Aurbach, *Russ. J. Electrochem.* 40 (2004) 273.
- [3] M.D. Levi, Y. Gofer, D. Aurbach, A. Berlin, *Electrochim. Acta* 49 (2004) 433.
- [4] G. Zotti, G. Schiavon, S. Zecchin, J.F. Morin, M. Leclerc, *Macromolecules* 35 (2002) 2122.
- [5] G. Zotti, S. Zecchin, B. Vercelli, A. Berlin, S. Grimoldi, M.C. Pasini, M.M.M. Raposo, *Chem. Mater.* 17 (2005) 6492.
- [6] D. Witker, J.R. Reynolds, *Macromolecules* 38 (2005) 7636.
- [7] R. Demadrille, B. Divisia-Blohorn, M. Zagorska, S. Quillard, P. Rannou, J.P. Travers, A. Pron, *New J. Chem.* 27 (2003) 1479.
- [8] Y. Diamant, E. Furmanovich, A. Landau, J.P. Lellouche, A. Zaban, *Electrochim. Acta* 48 (2003) 507.
- [9] N. Elming, N. Clauson-Kaas, *Acta Chem. Scand.* 6 (1952) 867.
- [10] S. Cosnier, S. Szunerits, R.S. Marks, J.P. Lellouche, K.J. Perie, *Biochem. Biophys. Methods* 50 (2001) 65.
- [11] W. Zhenhong, X. Jingcum, N. Guangming, D. Yukou, P.J. Shouzhi, *Electroanal. Chem.* 589 (2006) 112.
- [12] P. Marrec, C. Dano, N. Gueguen-Simonet, J. Simonet, *Synth. Met.* 89 (1997) 171.
- [13] Jerry March (Ed.), *Advanced Organic Chemistry: Reactions, Mechanisms and Structures*, fourth ed., Wiley-Interscience, John Wiley & Sons, 1992, p. 14 and p 17.
- [14] J. Garcia-Cañadas, F. Fabregat-Santiago, I. Porqueras, C. Person, J. Bisquert, G. Garcia-Belmonte, *Solid State Ionics* 175 (2004) 521.
- [15] G. Garcia-Belmonte, Z. Pomerantz, J. Bisquert, J.P. Lellouche, A. Zaban, *Electrochim. Acta* 49 (2004) 3413.
- [16] J. Tanguy, N. Mermilliod, M. Hocklet, *J. Electrochem. Soc.* 134 (1987) 795.
- [17] T.F. Otero, I. Boyano, *Chem. Phys. Chem.* 4 (2003) 868.
- [18] T.F. Otero, H. Grande, J. Rodriguez, *Synth. Met.* 83 (1996) 205.